Control of Underactuated Autonomous Underwater Vehicles With Input Saturation Based on Passivity Using Feedback Concavification

Shuyuan Fan and Herbert Werner

Abstract— **This paper aims to apply the concept of feedback concavification to the control of an underactuated autonomous underwater vehicle (AUV) with 6-DOF, subject to actuator saturation, to improve transient performance and robustness, taking into account the presence of unknown model dynamics and disturbances. To address the underactuated problem under the dissipation framework, Euclidean geometry is utilized to match the dimensions of the input and output. Therefore, an interconnected architecture for the AUV system is proposed, enabling the AUV system to be transformed into interconnected passive systems via feedback within this architecture with guaranteed asymptotic stability. The feedback concavification technique is then applied to the interconnected passive systems to handle uncertainties, disturbances, and actuator saturation problems. The proposed method with assigned concavity is effective in different scenarios with fast transient response and the decreasing L_2- gain under actuator saturation. Furthermore, the concept of concavity is incorporated into the proportion-derivative (PD) framework with the aim of enhancing the control performance. Numerical simulations have demonstrated the effectiveness of the proposed interconnected passive architecture and the feedback concavification approach in improving the control performance of the underactuated AUV. All the related files of this paper are available at [1].**

I. INTRODUCTION

In our related work [2], a novel concept known as feedback concavification is introduced with the concave closed-loop behavior and concave factors. This approach has two significant features: 1) the convergence rate increases as the control error decreases; 2) the L_2-gain from the disturbances or uncertainties to the control output decreases as the control error decreases. This approach is effective in enhancing the control performance in the presence of the actuator' saturation. The concept of feedback concavification is similar to the composite nonlinear feedback (CNF) technique [3] and the piecewise-linear LQ (PLQ) control [4]. These methods are effective in improving performance under input constraints. Nonetheless, CNF and PLQ methodologies emphasize the aspects of gain scheduling, whereas the feedback concavification concept directly targets the closed-loop behavior, furnishing a well-defined structure for the concave closed-loop system that delivers commendable control performance. This paper's objective is to broaden the application of this concept to the control of nonlinear systems, with a specific focus on its implementation for underactuated AUVs.

Shuyuan Fan is with the Institute of Control Systems, Hamburg University of Technology, Eissendorfer Str. 40, 21073 Hamburg, Germany shuyuan.fan@tuhh.de

Herbert Werner is with the Institute of Control Systems, Hamburg University of Technology, Eissendorfer Str. 40, 21073 Hamburg, Germany h.werner@tuhh.de

The underactuated AUV is a typical and highly used underactuated system. Underactuated AUVs are more widely used in practical applications because of the low energy consumption, cost, and weight compared to fully actuated AUVs and over-actuated AUVs [5]. The control of underactuated AUVs is still a challenging problem due to the presence of external disturbances, model uncertainties, coupling nonlinearities, underactuated characteristics and actuators' constraints (See [6]–[14] for the details). To address these issues, it's crucial to design a highly robust controller for AUV systems. Those research tend to opt for simplified numerical models such as 3-DOF, 4-DOF, and 5-DOF configurations. Nevertheless, it is crucial to emphasize that the complete 6-DOF dynamic model holds significant importance and offers a broader perspective in the field of AUVs [9]. Extending the control methods from the lower-DOF model to the higher-DOF model is tough. On the contrary, the control methods for 6-DOF model can be easily extended to the lower-DOF model by enforcing some states to be zero. For this purpose, this paper focuses on the underactuated 6-DOF dynamic model of a realistic mini-AUV developed and identified by TUHH [15]. There is some research on this model as shown in [16]–[18], where a PD controller is deployed, but without incorporating considerations for robustness. With that PD controller, it is difficult to take the other tough tasks [16]–[18]. This motivates the authors to design a robust controller with multiple functions.

The control system always requires the total energy to be dissipative to guarantee stability and control performance. Dissipation inequalities introduced by Willems in [19] are widely used for the analysis and design of interconnected nonlinear systems, particularly the passive system with the quadratic supply rate which is always utilized to guarantee the stability and robustness (L_2-gain), and the related theorem and techniques are fairly mature (See [20]–[22] for the details). Dissipativity describes input-output properties, and the associated supply rate is a one-dimensional map from input and output to the real number. Though the definition of a dissipative system does not explicitly require input and output to have the same dimensions, it is generally assumed when designing interconnected passive systems with quadratic supply rate, as presented in [22], [23]. However, due to the underactuated properties, the input dimension and the output (interconnection) dimension do not match. Thankfully, the Euclidean vector provides a way to transform a 3D vector into a one-dimensional vector together with a direction vector, which enables the underactuated AUV to unify the dimensions of input and output (interconnection). This inspired the authors to develop an interconnected passive architecture for underactuated AUVs. To enhance the robustness and transient response within the actuators' saturation, the concavity is introduced to the passive system with the help of the concave factor.

This paper offers two notable contributions. Firstly, it defines an interconnected passive structure for AUVs utilizing Euclidean vectors. Within this framework, it becomes straightforward to allocate and design performance (L2-gain) through the feedback methods. Secondly, it introduces feedback concavification techniques to tackle issues arising from uncertainties, disturbances, and actuator saturation. Simultaneously, these feedback concavification techniques serve to enhance the pre-existing PD controller. It is important to emphasize that concavity is determined in relation to the Lyapunov function rather than the system states.

Notation: Throughout this paper, the set $\mathbb{R}$ is the set of real number. $\mathbb{R}^n$ denotes the n-dimensional Euclidean space. $||\cdot||$ denotes the Euclidean norms. $\lambda(\cdot)$ denotes the eigenvalues of a square matrix $(\cdot)$. $\bar{\lambda}(\cdot)$ and $\underline{\lambda}(\cdot)$ denote the maximum and minimum eigenvalue of a square matrix $(\cdot)$, respectively. $M \prec (\succ) 0$ implies M is negative (positive) definite. $\dot{V} = \frac{\mathrm{d}V}{\mathrm{d}t}$. The set of real-valued square-integrable signals $u : [0,\infty) \to \mathbb{R}^m$ is denoted by $\mathcal{L}_2^m[0,\infty)$, with $\mathcal{L}_{2e}[0,\infty)$ denoting the associated extended signal space [22]. For a vector $\nu \in \mathbb{R}^3$, $\nu^* \in \mathbb{R}$ denotes the Euclidean distance by the notation *. For a Euclidean vector $\vec{a} := [a_1, a_2, a_3]^\top \in \mathbb{R}^3$, then define

$$\vec{a} = ||\vec{a}||\Gamma(\theta_a, \psi_a)$$

with

$$\Gamma(\theta_a, \psi_a) := \begin{bmatrix} \cos(\theta_a)\cos(\psi_a) \\ \cos(\theta_a)\sin(\psi_a) \\ -\sin(\psi_a) \end{bmatrix}$$

where $\theta_a := \operatorname{atan2}(-a_2, \sqrt{a_1^2 + a_2^2})$, $\psi_a := \operatorname{atan2}(a_2, a_1)$.

II. Underactuated AUV and Problem Formulation

A. Underactuated AUV Modeling

This paper considers the *Hippocampus*, an autonomous underwater vehicle developed at TUHH [15] with actuator saturation (See Fig.1). The 6-DOF mathematical representation of the AUV is derived and characterized in reference to [15], drawing from the well-known handbook on underwater vehicles [7]. It can be expressed as follows:

$$\begin{aligned} \dot{\eta} &= J(\Theta)\boldsymbol{v} \\ M\dot{\boldsymbol{v}} &= -C(\boldsymbol{v})\boldsymbol{v} - D(\boldsymbol{v})\boldsymbol{v} - g(\eta) + \tau_d + \tau \end{aligned} \tag{1}$$

where $\eta = [\ X \ \ \Theta\ ]^\top$, $\boldsymbol{v} = [\ \nu \ \ \omega\ ]^\top$. $X = [\ x \ \ y \ \ z\ ]^\top$ is the position vector which represents the distance from the inertial frame $\{n\}$ to the body fixed frame $\{b\}$, expressed in NED coordinates (See Fig.1) and $\Theta = [\ \phi \ \ \theta \ \ \psi\ ]^\top$ is the orientation vector which denotes the three Euler angles in three-dimensional space. $\nu = [\ u \ \ v \ \ w\ ]^\top$ describes the linear velocity and

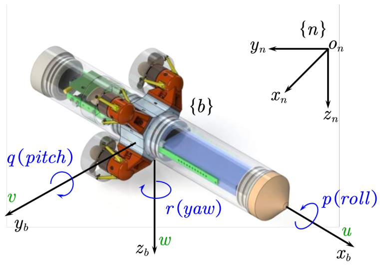

Fig. 1. 6 DOF velocities u, v, w, p, q and r in the body-fixed frame $\{b\}$ of the Hippocampus and inertial reference frame $\{n\}$

$\omega = [\ p \ \ q \ \ r\ ]^\top$ denotes the angular velocity. $\tau_d \in \mathbb{R}^6$ denotes the uncertainties and disturbance and $\boldsymbol{\tau} = [\ f \ \ 0 \ \ 0 \ \ \tau_{roll} \ \ \tau_{pitch} \ \ \tau_{yaw}\ ]^\top$ denotes the control input vector with underactuated property, which includes the thrust force f and three moments τ_{roll}, τ_{pitch}, τ_{yaw}. Define $\tau_s := [\ f \ \ \tau_{roll} \ \ \tau_{pitch} \ \ \tau_{yaw}\ ]^\top$, then τ_s satisfies the saturation as follows

$$\tau_s = L\mathrm{Sat}(\mathcal{T}) \tag{2}$$

where $\mathcal{T} \in \mathbb{R}^4$ is the torque vector of four deployed motors, and L is a matrix map from the torque vector to the input vector τ_s. The saturation function is defined as

$$\mathrm{Sat}(\mathcal{T}_i) = \begin{cases} \bar{\mathcal{T}}_i & \text{for } \ \mathcal{T}_i > \bar{\mathcal{T}}_i \\ \mathcal{T}_i & \text{for } \ -\bar{\mathcal{T}}_i \le \mathcal{T}_i \le \bar{\mathcal{T}}_i \\ -\bar{\mathcal{T}}_i & \text{for } \ \mathcal{T}_i < -\bar{\mathcal{T}}_i \end{cases} \quad i = 1,2,3,4 \tag{3}$$

$\boldsymbol{J}(\boldsymbol{\eta}) = \operatorname{diag}(R(\boldsymbol{\Theta}), T(\boldsymbol{\Theta}))$ is the block diagonal matrix consisting of the linear velocity transformation matrix $R(\boldsymbol{\Theta})$ between $\{b\}$ and $\{n\}$, and the angular velocity transformation matrix $T(\boldsymbol{\Theta})$, where

$$R(\boldsymbol{\Theta}) = \begin{bmatrix} c_\psi c_\theta & -s_\psi c_\phi + c_\psi s_\theta s_\phi & s_\psi s_\phi + c_\psi s_\theta c_\phi \\ s_\psi c_\theta & c_\psi c_\phi + s_\psi s_\theta s_\phi & -c_\psi s_\phi + s_\psi s_\theta c_\phi \\ -s_\theta & c_\theta s_\phi & c_\theta c_\phi \end{bmatrix}$$

$$T(\boldsymbol{\Theta}) = \begin{bmatrix} 1 & s_\phi t_\theta & c_\phi t_\theta \\ 0 & c_\phi & -s_\phi \\ 0 & s_\phi / c_\theta & c_\phi / c_\theta \end{bmatrix}$$

and $s.$, $c.$, $t.$ denote $\sin(\cdot)$, $\cos(\cdot)$, $\tan(\cdot)$, respectively. M represents the combined mass matrix, $C(\boldsymbol{v}) \in \mathbb{R}^{6\times 6}$ represents the matrix of Coriolis effects, $D(\boldsymbol{v}) \in \mathbb{R}^{6\times 6}$ is the hydrodynamic damping matrix, and $g(\eta) \in \mathbb{R}^6$ describes the hydrostatic load for a neutrally buoyant underwater vehicle. Those values are determined experimentally by [24].

B. Problem Formulation

Assume the underactuated AUV can reach and track a position reference trajectory $X_{ref}(t) \in \mathbb{R}^3$ starting from any initial position states $X(0)$. The maximum velocity of the AUV model is constrained by the actuator saturation. Thus, the comprehensive velocity of $X_{ref}(t)$ should within this constraints. Considering the numerical dynamic model (1) with the unknown disturbance τ_d, design τ under the input saturation (3) so that the underactuated AUV can converge to the reference trajectory such that .

$$\lim_{t\to\infty} ||X(t) - X_{ref}(t)|| \leq \delta \tag{4}$$

where δ is positive and arbitrarily small.

III. Passivity and Concave Closed-Loop Systems

A. Dissipativity and Passivity

Consider the continuous-time nonlinear system as follows

$$\Sigma : \begin{cases} \dot{x} = f(x,u) \\ y = h(x) \end{cases} \tag{5}$$

with state $x \in \mathcal{X} \subseteq \mathbb{R}^n$, input $u \in \mathcal{U} \subseteq \mathbb{R}^m$ and output $y \in \mathcal{Y} \subseteq \mathbb{R}^m$. The maps f and h are assumed to be sufficiently smooth and all input functions $u(\cdot), y(\cdot) \in \mathcal{L}_{2e}^m[0,\infty)$. The system is assumed to be fully controllable for all $x \in \mathcal{X}$. Moreover, we assume $f(0,0) = 0$ and $h(0) = 0$, such that $(u_e, x_e, y_e) = (0,0,0)$ is an equilibrium. We adopt and condense the relevant definitions of dissipativity from [22], [23].

Definition 1. *Let $s : \mathcal{U}\times\mathcal{Y} \to \mathbb{R}$ define a continuous function called the supply rate. The system Σ is dissipative with respect to the supply rate $s(u,y)$ if there exists a continuously differentiable storage function $V(x) \geq 0$ with $V(0) = 0$, such that the following dissipation inequality holds*

$$\frac{\mathrm{d}}{\mathrm{d}t}V(x) \leq s(u,y). \tag{6}$$

In this paper, we focus on passive systems with quadratic supply rates. Different from the original definition of passivity presented in [22], we extend it to the dissipation with the general quadratic supply rates.

Definition 2. *Consider the quadratic supply rates*

$$s(u,y) = \begin{bmatrix} y \\ u \end{bmatrix}^\top \begin{bmatrix} Q & S^\top \\ S & R \end{bmatrix} \begin{bmatrix} y \\ u \end{bmatrix} \tag{7}$$

where $Q = Q^\top \in \mathbb{R}^{m\times m}$, $S \in \mathbb{R}^{m\times m}$ and $R = R^\top \in \mathbb{R}^{m\times m}$ are square matrices. Suppose Σ is dissipative with respect to the quadratic supply rate (7). Σ is passive if $Q = 0, S \neq 0, R = 0$; Σ is input strictly passive if $Q = 0, R \prec 0$; Σ is output strictly passive if $Q \prec 0, R = 0$; if $Q = -I_m, R = \gamma^2 I_m, S = 0$ for $\gamma > 0$, then Σ has finite L_2-gain $G(y,u) \leq \gamma$.

This paper will take advantage of the output strictly passive system for the controller design.

Proposition 1. *Σ has the L_2-gain $G(y,u) \leq \frac{2\sqrt{\bar{\lambda}(SS^\top)}}{\underline{\lambda}(-Q)}$ if it is output strictly passive.*

Proof: Based on the definitions, we have the dissipation inequality

$$\begin{aligned}
&\frac{\mathrm{d}}{\mathrm{d}t}V(x) \leq 2u^\top Sy + y^\top Qy \leq 2u^\top Sy - \underline{\lambda}(-Q)||y||^2 \\
&\quad\leq 2u^\top Sy - \underline{\lambda}(-Q)||y||^2 + \left\| \sqrt{\frac{2}{\underline{\lambda}(-Q)}} S^\top u - \sqrt{\frac{\underline{\lambda}(-Q)}{2}} y \right\|^2 \\
&\quad= \frac{2}{\underline{\lambda}(-Q)} u^\top SS^\top u - \frac{1}{2}\underline{\lambda}(-Q)||y||^2 \\
&\quad\leq \frac{2\bar{\lambda}(SS^\top)}{\underline{\lambda}(-Q)}||u||^2 - \frac{1}{2}\underline{\lambda}(-Q)||y||^2 \\
&\quad= \frac{\underline{\lambda}(-Q)}{2}\left(\left(\frac{2\sqrt{\bar{\lambda}(SS^\top)}}{\underline{\lambda}(-Q)} \right)^2 ||u||^2 - ||y||^2 \right)
\end{aligned}$$

which implies Σ has the L_2-gain $G(y,u) \leq \frac{2\sqrt{\bar{\lambda}(SS^\top)}}{\underline{\lambda}(-Q)}$.

B. Concave Closed-Loop System and Concave Output Strict Passivity

Recall the definition of the concave closed-loop system first introduced in [2] as follows.

Definition 3. *Assume a smooth control law $u(x)$ is stabilizing system (5), such that the closed-loop system*

$$\dot{x} = f_{cl}(x) \tag{8}$$

where $f_{cl}(x)$ is Lipschitz. Assume V is a Lyapunov function of (8) and its derivative

$$\dot{V} = -x^\top M_{cl}(x)x \tag{9}$$

where $M_{cl}(x) \succ 0$ and $M_{cl}(x)$ is bounded. If and only if $x^\top M_{cl}(x)x$ is concave with respect to V, then the system (8) is called to be a concave closed-loop system.

Consider the quadratic form Lyapunov function $V = x^\top Px (P \succ 0)$, then the following conditions hold

$$\frac{\mathrm{d}M_{cl}(x)}{\mathrm{d}t} \succ 0, \quad \frac{\mathrm{d}M_{cl}(x)}{\mathrm{d}V} \prec 0 \tag{10}$$

and the $M_{cl}(x)$ is called to be a concave factor matrix with respect to V.1

To further analyze the benefits of the concave closed-loop system, let's reconsider the closed-loop system (8) with disturbance or systems uncertainties $\Delta \in \mathbb{R}^n$, such that

$$\begin{cases} \dot{x} = f_{cl}(x) + \Delta \\ y = h(x) := x \end{cases} \tag{11}$$

We have the following proposition.

Proposition 2. *The concave closed-loop system has two significant properties as follows*

- *The convergence rate increases as the control error V decreases.*
- *The L_2-gain from Δ to the control output y denoted by $G(y,\Delta)$ decreases as the control error V decreases.*

Proof: Assume $\Delta = 0$ for the evaluation of the transient performance. Due to

$$\dot{V} \leq -\underline{\lambda}(M_{cl}(x))x^\top x$$

then the large $\lambda(M_{cl}(x))$ means the larger convergence rate. Since $\frac{\mathrm{d}M_{cl}(x)}{\mathrm{d}V} \prec 0$, then we have $\frac{\mathrm{d}\lambda_i(M_{cl}(x))}{\mathrm{d}V} < 0 \quad (i = 1, \cdots, n)$, which implies the convergence rate increases as V decreases.

Assume $\Delta \neq 0$ for the evaluation of the performance of disturbance rejection. Then

$$\begin{aligned}
\dot{V} &= -x^\top M_{cl}(x)x + 2x^\top P\Delta \leq -\underline{\lambda}(M_{cl}(x))\,\|y\|^2 + 2\Delta^\top Py \\
&\leq -\underline{\lambda}(M_{cl}(x))\,\|y\|^2 + 2\Delta^\top Py \\
&\quad + \left\| \sqrt{\frac{2}{\underline{\lambda}(M_{cl}(x))}}P\Delta - \sqrt{\frac{\underline{\lambda}(M_{cl}(x))}{2}}y \right\|^2 \\
&= -\frac{1}{2}\underline{\lambda}(M_{cl}(x))\,\|y\|^2 + \frac{2\bar{\lambda}(P)^2}{\underline{\lambda}(M_{cl}(x))}||\Delta||^2 \\
&\leq \frac{\underline{\lambda}(M_{cl}(x))}{2}\left(\left(\frac{2\bar{\lambda}(P)}{\underline{\lambda}(M_{cl}(x))}\right)^2 ||\Delta||^2 - ||y||^2\right)
\end{aligned}$$

which implies the closed-loop system (8) has L_2- gain $G(y,\Delta) \leq \frac{2\bar{\lambda}(P)}{\underline{\lambda}(M_{cl}(x))}$. Since $\frac{\mathrm{d}\underline{\lambda}(M_{cl}(x))}{\mathrm{d}V} \leq 0$, therefore $\frac{\mathrm{d}G(y,\Delta)}{\mathrm{d}V} > 0$. This implies the L_2-gain decreases as the control error V decreases.

Combining the output strict passivity and the concave closed-loop behavior, we propose the concept of a concave output strictly passive system.

Definition 4. *For a system as (5), if it is dissipative with respect to the supply rate*

$$s(u, y) = u^\top Sy + y^\top Q(x)y$$

with the storage function V where $-Q(x) \succ 0$ is a concave factor matrix with respect to the storage function V (V has the quadratic form) that

$$\frac{\mathrm{d}(-Q(x))}{\mathrm{d}t} \succ 0, \quad \frac{\mathrm{d}(-Q(x))}{\mathrm{d}V} \prec 0$$

then it is called to be concave output strictly passive.

Here, we introduce two useful concave functions as follows

1) Root-Like Concave function: Root functions ($\rho^\alpha, 0 < \alpha < 1$) are widely used in sliding mode control and finite-time convergence control. However, it is not smooth around the origin. By abusing the notation, we introduce a framework of root-like concave functions as follows.

$$F(\rho) = \underbrace{\frac{\rho^{\alpha_1} + \beta_1}{\rho^{\alpha_2} + \beta_2}}_{f_c}\rho \quad (\alpha_1, \alpha_2, \beta_1 \geq 0, \beta_2 > 0, \rho \geq 0) \quad (12)$$

where $0 < \alpha_2 - \alpha_1 < 1$. Selecting proper β_1, β_2, we can ensure $F(\rho)$ to be strictly concave in the domain (ϵ, ρ_{max}) where $\epsilon > 0$ is relatively small. Moreover, f_c is called to be a concave factor and ρ denotes the control error like Lyapunov function.

2) Slider-like concave function: We assume that a larger control gain k_{max} to ensure the performance and a minimum gain k_{min} to satisfy the input saturation. The role of the concave factor is adjusting the control gain from the k_{min} to k_{max} under the actuator's saturation. Consequently, we propose the following concave function.

$$F(\rho) = \underbrace{\frac{\beta_1 k_{min}\rho^\alpha + \beta_2 k_{max}}{\beta_1\rho^\alpha + \beta_2}}_{f_c}\rho \quad (\beta_1, \beta_2 > 0, 0 < \alpha \leq 1) \quad (13)$$

where β_1, β_2 can shift the sliding speed from k_{min} to k_{max} with the decrease of ρ.

IV. Controller Design

A. The Interconnected Architecture for AUV With the Reduced Dimension

Without any simplification, we can split the whole system (1) into four subsystems, such that

$$\Sigma_1: \begin{cases} \dot{X} = R(\Theta)\nu \\ y_1 = h_1(X) \end{cases}$$

$$\Sigma_2: \begin{cases} M_1\dot{\nu} = -C_1(\nu)\omega - D_1(\nu)\nu - g_1(\eta) + \tau_{d1} + \tau_1 \\ y_2 = h_2(\nu) \end{cases}$$

$$\Sigma_3: \begin{cases} \dot{\Theta} = T(\Theta)\omega \\ y_3 = h_3(\Theta) \end{cases}$$

$$\Sigma_4: \begin{cases} M_2\dot{\omega} = -C_1(\nu)\nu - C_2(\omega)\omega - D_2(\omega)\omega - g_2(\eta) + \tau_{d2} + \tau_2 \\ y_4 = h_4(\omega) \end{cases}$$

where

$$C(\upsilon) = \begin{bmatrix} 0_{3\times3} & C_1(\nu) \\ C_1(\nu) & C_2(\omega) \end{bmatrix} \quad D(\upsilon) = \begin{bmatrix} D_1(\nu) & 0_{3\times3} \\ 0_{3\times3} & D_2(\omega) \end{bmatrix}$$

where $C_1(\nu), C_2(\omega) \in \mathbb{R}^{3\times3}$ are skew-symmetric matrices, $M = \mathrm{diag}(M_1, M_2)$ with $M_1, M_2 \succ 0 \in \mathbb{R}^{3\times3}$, $g(\eta) = [g_1(\eta), g_2(\eta)]^\top$ with $g_1(\eta), g_2(\eta) \in \mathbb{R}^3$,$\tau_d = [\tau_{d_1}, \tau_{d_2}]^\top$ with $\tau_{d_1}, \tau_{d_2} \in \mathbb{R}^3$,$\tau_d = [\tau_1, \tau_2]^\top$ with $\tau_1, \tau_2 \in \mathbb{R}^3$. Due to the underactuated properties $\tau_1 = [f, 0, 0]^\top$, the dimension condition $y_2 \in \mathbb{R}$ should hold to assign a passive system. Moreover, the interconnection between Σ_1 and Σ_2 should be reduced to be one dimensional. Those two conditions are necessary to obtain passive interconnected systems according to the Definition 2. Then, define

$$\nu := \Gamma(\theta_\nu, \psi_\nu)\nu^* \qquad \tau_{d_1} := \Gamma(\theta_{\tau_{d_1}}, \psi_{\tau_{d_1}})\tau^*_{d_1}$$

where $\nu^*, \tau^*_{d_1} \in \mathbb{R}$. Define the interconnection that $y_2 := \nu^*$, $y_3 := \Theta$, $y_4 := \omega$, then we can obtain an interconnected system as shown in Fig.2. Moreover, y_1 should be designed later.

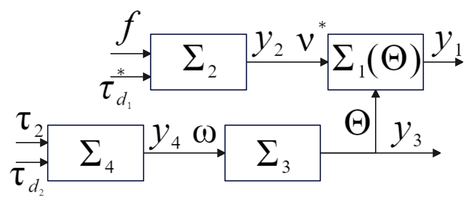

Fig. 2. The equivalent interconnected system

B. Passivity by Feedback

We first transform the four interconnected subsystems $\Sigma_1, \Sigma_2, \Sigma_3, \Sigma_4$ into four passive interconnected subsystems denoted by $\Sigma_1^p, \Sigma_2^p, \Sigma_3^p, \Sigma_4^p$ by feedback.

1) Passivity for Σ_1*:* let $\nu^* := \nu_f^* + \nu_e^*$ that ν_f^* denotes the feedback part and ν_e^* denotes the external input. Assume system Σ_1^p is dissipative with respect to the supply rate $s(\nu_e^*, y_1) := \nu_e^* S_1 y_1 + Q_1 y_1^2$ with the storage function $V_1 := \frac{1}{2} X^\top X$.

$$\begin{aligned}\frac{\mathrm{d}}{\mathrm{d}t} V_1 &= (\nu_e^* + \nu_f^*)^\top \Gamma^\top(\theta_\nu, \psi_\nu) R^\top(\Theta) X \\ &= \nu_e^* \Gamma^\top(\theta_\nu, \psi_\nu) R^\top(\Theta) X + \nu_f^* \Gamma^\top(\theta_\nu, \psi_\nu) R^\top(\Theta) X \\ &\leq \nu_e^* S_1 y_1 + Q_1 y_1^2\end{aligned}$$

Then, we can define $S_1 := 1$, $y_1 := \Gamma^\top(\theta_\nu, \psi_\nu) R^\top(\Theta) X$ and $\nu_f^* = Q_1 y_1$ with $Q_1 < 0$. Thus, it becomes a passive system Σ_1^p with the external input ν_e^*. To obtain a concave passive system, we can design $-Q_1$ as a concave factor with respect to the storage function V_1.

2) Passivity for Σ_2*:* Due to the interconnection $y_2 = \nu_f^* + \nu_e^*$, then $\nu_e^* := y_2 - \nu_f^*$. To connect the passive system Σ_1^p, define the new connection $\hat{y}_2 := \nu_e^*$. Assume system Σ_2^p is dissipative with respect to the supply rate $s(\tau_{d_1}^*, \hat{y}_2) := \tau_{d_1}^* S_2 \hat{y}_2 + \hat{y}_2^\top Q_2 \hat{y}_2$ with the storage function $V_2 := \frac{1}{2} \hat{y}_2 \Gamma^\top(\theta_\nu, \psi_\nu) M_1 M_1 \Gamma(\theta_\nu, \psi_\nu) \hat{y}_2$. Then

$$\begin{aligned}\frac{\mathrm{d}V_2}{\mathrm{d}t} =& \underbrace{(-C_1(\nu)\omega - D_1(\nu)\nu - g_1(\eta) - \frac{\mathrm{d}M_1\Gamma(\theta_\nu, \psi_\nu)\nu_f^*}{\mathrm{d}t}}_{H} \\ & + \tau_{d_1}^* \Gamma(\theta_{\tau_{d_1}}, \psi_{\tau_{d_1}}))^\top M_1 \Gamma(\theta_\nu, \psi_\nu) \hat{y}_2 \\ & + f \Gamma^\top(0,0) M_1 \Gamma(\theta_\nu, \psi_\nu) \hat{y}_2 \\ =& H^\top M_1 \Gamma(\theta_\nu, \psi_\nu) \hat{y}_2 + f \Gamma^\top(0,0) M_1 \Gamma(\theta_\nu, \psi_\nu) \hat{y}_2 \\ & + \tau_{d_1}^* \Gamma^\top(\theta_{\tau_{d_1}}, \psi_{\tau_{d_1}}) M_1 \Gamma(\theta_\nu, \psi_\nu) \hat{y}_2 \\ & \leq \tau_{d_1}^* S_2 \hat{y}_2 + Q_2 \hat{y}_2^2\end{aligned}$$

Assume $S_2 = \Gamma^\top(\theta_{\tau_{d_1}}, \psi_{\tau_{d_1}}) M_1 \Gamma(\theta_\nu, \psi_\nu)$. Then, define

$$H^\top M_1 \Gamma(\theta_\nu, \psi_\nu) + f \Gamma^\top(0,0) M_1 \Gamma(\theta_\nu, \psi_\nu) = Q_2 \hat{y}_2 \quad (14)$$

Solving equation (14), we obtain the solution

$$f = \frac{Q_2 \hat{y}_2 - H^\top M_1 \Gamma(\theta_\nu, \psi_\nu)}{\Gamma^\top(0,0) M_1 \Gamma(\theta_\nu, \psi_\nu)} \quad (\cos(\theta_\nu)\cos(\psi_\nu) \neq 0) \quad (15)$$

Clearly, $\cos(\theta_\nu)\cos(\psi_\nu) = 0$ if and only if $u = 0, v^2 + w^2 \neq 0$. Generally speaking, $-\frac{\pi}{4} \leq \theta_\nu, \psi_\nu \leq \frac{\pi}{4}$ due to v, w come from the Coriolis effect.

3) Passivity for Σ_3*:* Although Σ_1^p is output strictly passive, the asymptotic stability can not be guaranteed, which is related to the configuration of Θ. Assume the configuration $\Theta_d(t)$ is sufficient to achieve the asymptotic stability. Define $\hat{y}_3 := y_3 - \Theta_d(t)$. Let $\omega := \omega_f + \omega_e$ where ω_f is a feedback part for the passivity and ω_e denotes the external input. Assume Σ_3^p is dissipative with respect to the supply rate $s(\omega_e, \hat{y}_3) := \omega_e^\top S_3 \hat{y}_3 + \hat{y}_3^\top Q_3 \hat{y}_3$ with the storage function $V_3 := \frac{1}{2} \hat{y}_3^\top \hat{y}_3$. Then

$$\begin{aligned}\frac{\mathrm{d}}{\mathrm{d}t} V_3 &= \omega_e^\top T^\top(\Theta) \hat{y}_3 + \omega_f^\top T^\top(\Theta) \hat{y}_3 - (\frac{\mathrm{d}\Theta_d(t)}{\mathrm{d}t})^\top \hat{y}_3 \\ &\leq \omega_e^\top S_3 \hat{y}_3 + \hat{y}_3^\top Q_3 \hat{y}_3\end{aligned}$$

Hence, we can define $S_3 := T^\top(\Theta)$

$$\omega_f := T^{-1}(\Theta) \left(Q_3 \hat{y}_3 + \frac{\mathrm{d}\Theta_d(t)}{\mathrm{d}t} \right)$$

with $Q_3 \prec 0$.

4) Passivity for Σ_4*:* Let ω_e be the connection between Σ_3^p and Σ_4^p. Then define $\hat{y}_4 := \omega_e$. Assume Σ_4^p is dissipative with respect to the supply rate $s(\tau_{d_2}, \hat{y}_4) := \tau_{d_2}^\top S_4 \hat{y}_4 + \hat{y}_4^\top Q_4 \hat{y}_4$ with the storage function $V_4 := \frac{1}{2} \hat{y}_4^\top M_2 M_2 \hat{y}_4$. Therefore,

$$\begin{aligned}\frac{\mathrm{d}}{\mathrm{d}t} V_4 &= O^\top M_2 \hat{y}_4 + \tau_{d_2}^\top M_2 \hat{y}_4 - (\frac{\mathrm{d}\omega_f}{\mathrm{d}t})^\top M_2 M_2 y_4^* + \tau_2^\top M_2 \hat{y}_4 \\ &\leq \tau_{d_2}^\top S_3 \hat{y}_4 + \hat{y}_4^\top Q_4 \hat{y}_4\end{aligned}$$

with $O := -C_1(\nu)\nu - C_2(\omega)\omega - D_2(\omega)\omega - g_2(\eta)$. Then we can define $S_4 := M_2$ and $M_2 O - M_2 M_2 \frac{\mathrm{d}\omega_f}{\mathrm{d}t} + M_2 \tau_2 = Q_4 \hat{y}_4$. Hence,

$$\tau_2 = M_2^{-1}(Q_4 \hat{y}_4 - M_2 O + M_2 M_2 \frac{\mathrm{d}\omega_f}{\mathrm{d}t}) \quad (16)$$

with $Q_4 \prec 0$.

Thus, we obtain the control law based on the passivity such that

$$\tau_s = \begin{bmatrix} f \\ \tau_2 \end{bmatrix} = \begin{bmatrix} \frac{Q_2 \hat{y}_2 - H^\top M_1 \Gamma(\theta_\nu, \psi_\nu)}{\Gamma^\top(0,0) M_1 \Gamma(\theta_\nu, \psi_\nu)} \\ M_2^{-1}(Q_4 \hat{y}_4 - M_2 O + M_2 M_2 \frac{\mathrm{d}\omega_f}{\mathrm{d}t}) \end{bmatrix}. \quad (17)$$

Consequently, we can obtain the interconnected passive system (Σ_{all}^p) as shown in Fig.3 Hence, Σ_{all}^p is dissipative

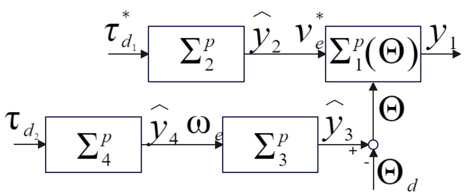

Fig. 3. The equivalent interconnected passive system (Σ_{all}^p)

with respect to the supply rate $s_{all} := s_1 + s_2 + s_3 + s_4$ with the storage function $V_{all} := V_1 + V_2 + V_3 + V_4$.

C. Stability Analysis

1) Stability when $\tau_d = 0$*:* For this case, we have

$$\frac{\mathrm{d}V_{all}}{\mathrm{d}t} = \begin{bmatrix} y_1 \\ \hat{y}_2 \end{bmatrix}^\top \begin{bmatrix} Q_1 & \frac{S_1^\top}{2} \\ \frac{S_1}{2} & Q_2 \end{bmatrix} \begin{bmatrix} y_1 \\ \hat{y}_2 \end{bmatrix} + \begin{bmatrix} \hat{y}_3 \\ \hat{y}_4 \end{bmatrix}^\top \begin{bmatrix} Q_3 & \frac{S_3^\top}{2} \\ \frac{S_3}{2} & Q_4 \end{bmatrix} \begin{bmatrix} \hat{y}_3 \\ \hat{y}_4 \end{bmatrix} \quad (18)$$

Let $Z := [X^\top, \Theta^\top, \nu^\top, \omega^\top]^\top$ denote the whole state vector and $\hat{Z} = 0$ is a stable equilibrium. Let $Y := [y_1, \hat{y}_2, \hat{y}_3^\top, \hat{y}_4^\top]^\top$ denote the output vector of the subsystems.

Proposition 3. *Suppose* $\Gamma^\top(\theta_\nu, \psi_\nu) R^\top(\Theta) \Gamma^\top(\theta_X, \psi_X) \neq 0$ *holds* $\forall Z \neq \hat{Z}$. *The Hippocampus is asymptotically stable at* $\hat{Z}$*, if* $\begin{bmatrix} Q_1 & \frac{S_1^\top}{2} \\ \frac{S_1}{2} & Q_2 \end{bmatrix} \prec 0$, $\begin{bmatrix} Q_3 & \frac{S_3^\top}{2} \\ \frac{S_3}{2} & Q_4 \end{bmatrix} \prec 0$*, and* $\Theta_d = 0$ *holds if* $y_1 = 0$.

Proof: Obviously, $\forall X$, $V_{all} \geq 0$ and $V_{all} = 0$ holds if and only if $Y = 0$. Since $\begin{bmatrix} Q_1 & \frac{S_1^\top}{2} \\ \frac{S_1}{2} & Q_2 \end{bmatrix} \prec 0$, $\begin{bmatrix} Q_3 & \frac{S_3^\top}{2} \\ \frac{S_3}{2} & Q_4 \end{bmatrix} \prec 0$, then $\lim_{t\to\infty} Y = 0$. Since $y_1 = 0$, then $\Theta_d(t) = 0$. This implies $\Theta = 0$. Then $\lim_{t\to\infty} Z = \hat{Z}$. This completes the proof.

Thus, to avoid $\Gamma^\top(\theta_\nu, \psi_\nu) R^\top(\Theta) \Gamma^\top(\theta_X, \psi_X) = 0$, we can design

$$\Theta_d(t) = \begin{bmatrix} 0 & -\theta_X & \psi_X - \pi \end{bmatrix}^\top \tag{19}$$

2) For $\tau^*_{d_1} \neq 0, \tau_{d_2} \neq 0$: For this case, similar, we have

$$\frac{\mathrm{d}V_{all}}{\mathrm{d}t} = \begin{bmatrix} y_1 \\ \hat{y}_2 \\ \tau^*_{d_1} \\ \hat{y}_3 \\ \hat{y}_4 \\ \tau_{d_2} \end{bmatrix}^\top \underbrace{\begin{bmatrix} Q_1 & \frac{S_1^\top}{2} & * & * & * & * \\ \frac{S_1}{2} & Q_2 & \frac{S_2^\top}{2} & * & * & * \\ * & \frac{S_2}{2} & * & * & * & * \\ * & * & * & Q_3 & \frac{S_3^\top}{2} & * \\ * & * & * & \frac{S_3}{2} & Q_4 & \frac{S_4^\top}{2} \\ * & * & * & * & \frac{S_4}{2} & * \end{bmatrix}}_{\Pi} \begin{bmatrix} y_1 \\ \hat{y}_2 \\ \tau^*_{d_1} \\ \hat{y}_3 \\ \hat{y}_4 \\ \tau_{d_2} \end{bmatrix}$$

where $(*)$ denotes the zero matrix with appropriate dimensions. If the disturbance weight S_2, S_4 satisfies $\Pi \prec 0$, then the system is asymptotically stable under the same condition of Proposition 3. If S_2, S_4 are available, then it is easy to solve Q_1, Q_2, Q_3, Q_4 satisfying $\Pi \prec 0$. If S_2, S_4 are unknown, we can obtain the L_2-gain from the disturbance or uncertainties to the output Y such that

$$G(Y, \begin{bmatrix} \tau_{d_1} \\ \tau_{d_2} \end{bmatrix}) \leq \max(\frac{S_1}{-Q_1}, \frac{S_2}{-Q_2}, \frac{\sqrt{\bar{\lambda}(S_3 S_3^\top)}}{\underline{\lambda}(-Q_3)}, \frac{\sqrt{\bar{\lambda}(S_4 S_4^\top)}}{\underline{\lambda}(-Q_4)}) \tag{20}$$

D. Trajectory Tracking

The passivity-based controller is originally designed for stabilizing control. We are now expanding its application to include set-point stabilization and trajectory tracking control. Let $Z_{ref} := [X_{ref}^\top, \Theta_{ref}^\top, \nu_{ref}^\top, \omega_{ref}^\top]^\top$ denote the reference state vector.

1) Set-point stabilizing control: For this case, we have $\frac{\mathrm{d}Z_{ref}}{\mathrm{d}t} = 0$ and $\nu_{ref} = 0, \omega_{ref} = 0$. Therefore, we use the following transformation

$$\begin{aligned} \hat{y}_1^{sp} &:= \Gamma^\top(\theta_\nu, \psi_\nu) R^\top(\Theta)(X - X_{ref}) \\ \hat{y}_3^{sp} &:= y_3 - \Theta_d(t) - \Theta_{ref} \end{aligned} \tag{21}$$

and then replace $y_1, \hat{y}_3$ with the set-point output $\hat{y}_1^{sp}, \hat{y}_3^{sp}$.

2) Trajectory tracking: For the trajectory tracking, first of all, we should obtain a trajectory denoted by $Z_{ref}(t)$ in advance. Generally speaking, the whole trajectory $Z_{ref}(t)$ is planned based on the location trajectory $X_{ref}(t)$. Due to the trajectory planning is embedded in the controller for handling the underactuated problem, thus, we assume $\Theta_{ref} = 0, \nu_{ref} = 0, \omega_{ref} = 0$ and only consider $X_{ref}(t)$. Similar to the set-point controller, we define

$$\begin{aligned} \hat{y}_1^{tk} &:= \Gamma^\top(\theta_\nu, \psi_\nu) R^\top(\Theta)(X - X_{ref}(t)) \\ V_1^{tk} &:= \frac{1}{2}(X - X_{ref}(t))^\top (X - X_{ref}(t)) \end{aligned} \tag{22}$$

Taking the derivative, we have

$$\begin{aligned} \frac{\mathrm{d}V_1^{tk}}{\mathrm{d}t} &= (R(\Theta)\nu - \frac{\mathrm{d}X_{ref}(t)}{\mathrm{d}t}))^\top (X - X_{ref}(t)) \\ &= \nu_f^* y_1^{tk} + \nu_e^* \hat{y}_1^{tk} + \nu_{ref}^* S_{ref} \hat{y}_1^{tk} \\ &= \left(\nu_f^* + \nu_{ref}^* S_{ref}\right) \hat{y}_1^{tk} + \nu_e^* \hat{y}_1^{tk} \end{aligned} \tag{23}$$

where

$$\begin{aligned} S_{ref} &= -\Gamma^\top(\theta_{\nu_{ref}}, \psi_{\nu_{ref}}) R(\Theta) \hat{\Gamma}_\nu^{-\top} \Gamma(\theta_\nu, \psi_\nu) \\ \hat{\Gamma}_\nu &:= \Gamma(\theta_\nu, \psi_\nu) \Gamma^\top(\theta_\nu, \psi_\nu) \\ \frac{\mathrm{d}X_{ref}(t)}{\mathrm{d}t} &= \nu_{ref}^* \Gamma(\theta_{\nu_{ref}}, \psi_{\nu_{ref}}) \end{aligned}$$

Remark 1. *On one hand, we can still adopt the set-point stabilizing control law and consider the derivative of the tracking reference $\dot{X}_{ref}(t)$ as the disturbance. Due to $S_{ref} \in \mathbb{R}$ and $S_{ref}^2 \leq 1$, then we can obtain the L_2-gain $G(\hat{y}_1^{tk}, \nu_{ref}^*)$ from ν_{ref}^* to the control output $\hat{y}_1^{tk}$ satisfying*

$$G(y_1^{tk}, \nu_{ref}^*) \leq \frac{1}{-Q_1}$$

Hence, to improve the performance, we can increase $-Q_1$.

Remark 2. *On the other hand, we can utilize the information of $\dot{X}_{ref}(t)$ and let $\nu_f^{*tk} = Q_1^{tk} \hat{y}_1^{tk} - \nu_{ref}^* S_{ref}$. Therefore, we obtain the control output $\hat{y}_2^{tk}$ of Σ_2^p for tracking*

$$\hat{y}_2^{tk} = y_2 - \nu_f^{tk} = y_2 - Q_1^{tk} \hat{y}_1^{tk} + \nu_{ref}^* S_{ref} \tag{24}$$

Replacing $y_1, \nu_f^*, \hat{y}_2$ with $\hat{y}_1^{tk}, \nu_f^{*tk}, \hat{y}_1^{tk}$, we can obtain the tracking control law.

V. Concavity for Enhancing the Control Performance in the Presence of the Actuator's Saturation

A. Concave Passivity

According to Proposition 3 and equation (20), the selection of the matrix $Q_i (i = 1, 2, 3, 4)$ is quite significant to enhance the control performance. In practical applications, the AUV's performance is often affected by uncertainties and disturbances. To reduce the L_2 gain caused by these disturbances on the control output, and enhance transient performance, it becomes necessary to increase the weight of $-Q_i$. However, if Q_i remains constant, a high $-Q_i$ value can strain the actuators and potentially lead to actuator saturation. To address this issue, we introduce the concept of concavity. Design $-Q_i$ as a concave factor matrix with respect to V_1 as follows

$$0 < k_{min}^i \leq \lambda(-Q_i) \leq k_{max}^i, \quad \frac{\mathrm{d}(-Q_i)}{\mathrm{d}V_i} < 0 \tag{25}$$

This implies, that the 'control gain' matrix $-Q_i$ increases as the control error decreases. Moreover, the small gain k_{min}^i is selected to satisfy the saturation, and the large gain k_{max}^i is designed to enhance the control performance.

B. Improve the PD Control Based On the Concave Factor

To demonstrate the effectiveness of the feedback concavification, we provide another comparison with a published controller on Hippocampus in [16]–[18], [25] which has been demonstrated via the experiment. We just replace the control gain with the concave factor. Thus, the improved PD controller

$$\tau_s^{PD} = \begin{bmatrix} K_u(K_{pos}||X_{ref} - X|| - u) \\ -K_R e_R - K_\omega(\omega_d - \omega) \end{bmatrix} \tag{26}$$

where $K_u > 0$, $K_R, K_\omega \succ 0$ are diagonal gain matrices. The other details are available at [16]–[18]. For the concave PD control, K_u is defined as a concave factor and K_R, K_ω are concave factor matrices.

VI. Numerical simulation

This section demonstrates the effectiveness of the feedback concavification concept and the proposed architecture of the interconnected passive systems in the application of the underactuated AUVs. All the simulation files of this paper are available at [1]. The detailed model parameters of $Hippocampus$ are published and available at [24]. The reference trajectory is infinity-shaped as follows

$$X_{ref}(t) = \begin{bmatrix} a_x \sin(\frac{\pi}{15}t) \\ a_y(\frac{\pi}{30}t) \\ 0.1t \end{bmatrix} \tag{27}$$

To evaluate the robustness, the disturbance is selected as $\tau_d := [0.2\sin(0.1t+1), 0.1\sin(0.15t+0.9), 0.1\sin(0.1t+0.5), 0.1\sin(0.05t+1), 0.1\sin(0.1t+2), 0.1\sin(0.15t+3)]^\top$. The parameters of the passive controller is designed as $Q_1 = -8$, $Q_2 = -10$, $Q_3 = -\text{diag}(0.01, 5, 8)$, $Q_4 = -\text{diag}(0.001, 0.1, 0.1)$. We select the slider-like concave factor to assign the concavity for the concave passive controller where the parameter $\alpha = 1$. Define $h := (k_{min}, k_{max}, \beta_1, \beta_2, \rho)$ as the parameters of function (13). Then, the parameters are given as follows

$$h_{Q_1} = (8, 50, 1, 0.01, V_1) \quad h_{Q_2} = (10, 80, 1, 0.02, V_2)$$
$$\begin{bmatrix} h^1_{Q_3} \\ h^2_{Q_3} \\ h^3_{Q_3} \end{bmatrix} = \begin{bmatrix} (0.01, 1, 1, 1, V_3) \\ (5, 20, 1, 0.01, V_3) \\ (8, 30, 1, 0.02, V_3) \end{bmatrix}$$
$$\begin{bmatrix} h^1_{Q_4} \\ h^2_{Q_4} \\ h^3_{Q_4} \end{bmatrix} = \begin{bmatrix} (0.001, 0.01, 1, 1, V_4) \\ (0.1, 10, 0.01, 0.02, V_4) \\ (0.1, 10, 0.01, 0.02, V_4) \end{bmatrix}$$

And the concave passive parameters $Q_1^c = -f_c(h_{Q_1})$, $Q_2^c = -f_c(h_{Q_2})$, $Q_3^c = -\text{diag}(f_c(h^1_{Q_3}), f_c(h^2_{Q_3}), f_c(h^3_{Q_3}))$,$Q_4^c = -\text{diag}(f_c(h^1_{Q_4}), f_c(h^2_{Q_4}), f_c(h^3_{Q_4}))$. For the PD controller, the parameters are selected as $K_{pos} = 8$, $K_u = 8$, $K_R = \text{diag}(10, 10, 10)$, $K_\omega = \text{diag}(1, 1, 1)$. For the concave PD controller, the parameters are selected as $h(K_{pos}) = (8, 20, 1, 0.01, ||X - X_{ref}||^2)$, $h(K_u) = h(K_{pos})$, $h(K_R^3) = (10, 20, 1, 0.01, e_R(3)^2)$ and $K^c_{pos} = K^c_u = f_c(h(K_{pos}))$, $K_R = \text{diag}(10, 10, f_c(h(K_R^3)))$, and $K^c_\omega = \text{diag}(1, 1, 1)$.

For a fair comparison, all the parameters of the above controller are well-tuned under the reference trajectory with $a_x = 4, a_y = 8$ when $\tau_d = 0$. Moreover, the limit of each motor is defined as $\bar{\mathcal{T}}_i = 3$. For $\tau_d = 0$, the tracking results are shown in Fig.4 and Fig.5. When $\tau_d = 0$, all controllers perform well. From Fig.5, we can find that the passive controller outperforms the PD controller, and the feedback concavification techniques can improve the tracking performance and reduce the tracking error under the input saturation.

Fig.6 and Fig.7 display the simulation results with $\tau_d \neq 0$. From Fig.6, we can observe that the PD controller becomes invalid when the disturbance is considering. However, the concave PD controller is still valid with good tracking performance. Furthermore, the passive controller consistently demonstrates reliable performance. It is evident that the feedback concavification techniques can significantly enhance tracking performance and robustness.

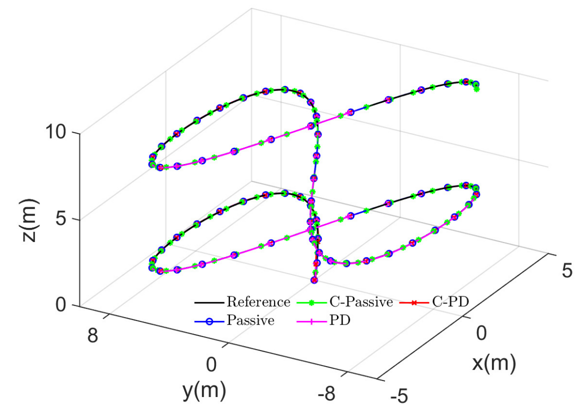

Fig. 4. Tracking results without disturbance where 'C-Passive' denotes the concave passive controller and 'C-PD' denotes the concave PD controller

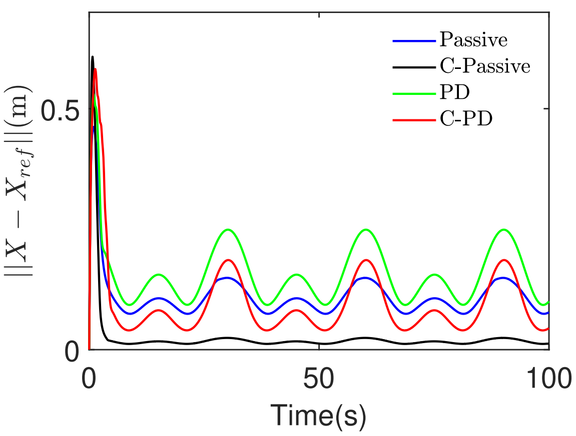

Fig. 5. Results of tracking error without disturbance

Remark 3. *We compared the controllers with different reference trajectories with different a_x, a_y. From those results, the concave passive controller consistently outperforms the other controllers. Nevertheless, sometimes, the PD controller becomes invalid when we change the reference. The adaptability and robustness of the concave passive controller are evident. One can check with the provided files in [1].*

VII. Conclusion

The paper introduces a novel approach for controlling underactuated Autonomous Underwater Vehicles (AUVs) using feedback concavification based on the passivity theorem. With the help of the Euclidean vector, an interconnected passive architecture of the 6-DOF underactuated AUV is proposed, simplifying the analysis and the assignment of closed-loop behavior. Simulation results effectively illustrate

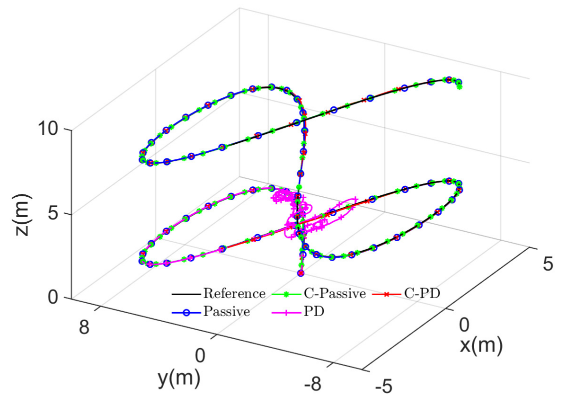

Fig. 6. Tracking results with disturbance

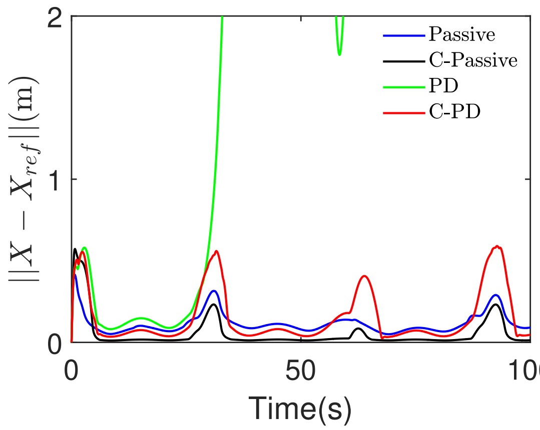

Fig. 7. Results of tracking error with disturbance

the effectiveness of this proposed passive structure for AUV control. After introducing the concavity, the control performance experiences a significant enhancement. The authors plan to further explore the potential of feedback concavification in other scenarios.

References

[1] S. Fan and H. Werner, "Control of underactuated autonomous underwater vehicles with input saturation based on passivity using feedback concavification," submitted to ECC. [Online]. Available: https://github.com/shuyuanfan/Hippocampus-Concavity.git

[2] S. F and H. Werner, "Feedback concavification techniques for enhangcing the transient performance and robustness for lti systems with input saturation," submitted to ECC. [Online]. Available: https://github.com/shuyuanfan/The-feedback-concavification.git

[3] M. P. Zongli Lin and S. Banda, "Toward improvement of tracking performance nonlinear feedback for linear systems," *International Journal of Control*, vol. 70, no. 1, pp. 1–11, 1998.

[4] G. Wredenhagen and P. Belanger, "Piecewise-linear lq control for systems with input constraints," *Automatica*, vol. 30, no. 3, pp. 403–416, 1994.

[5] M. J. Er, H. Gong, Y. Liu, and T. Liu, "Intelligent trajectory tracking and formation control of underactuated autonomous underwater vehicles: A critical review," *IEEE Transactions on Systems, Man, and Cybernetics: Systems*, 2023.

[6] L. Hong, R. Fang, X. Cai, and X. Wang, "Numerical investigation on hydrodynamic performance of a portable auv," *Journal of Marine Science and Engineering*, vol. 9, no. 8, p. 812, 2021.

[7] T. I. Fossen, *Handbook of marine craft hydrodynamics and motion control*. John Wiley & Sons, 2011.

[8] K. D. Do and J. Pan, *Control of ships and underwater vehicles: design for underactuated and nonlinear marine systems*. Springer, 2009, vol. 1.

[9] S. Bhat and I. Stenius, "Hydrobatics: A review of trends, challenges and opportunities for efficient and agile underactuated auvs," in *2018 IEEE/OES Autonomous Underwater Vehicle Workshop (AUV)*, 2018, pp. 1–8.

[10] F. Muñoz, J. S. Cervantes-Rojas, J. M. Valdovinos, O. Sandre-Hernández, S. Salazar, and H. Romero, "Dynamic neural network-based adaptive tracking control for an autonomous underwater vehicle subject to modeling and parametric uncertainties," *Applied Sciences*, vol. 11, no. 6, p. 2797, 2021.

[11] C. Wang, W. Cai, J. Lu, X. Ding, and J. Yang, "Design, modeling, control, and experiments for multiple auvs formation," *IEEE Transactions on Automation Science and Engineering*, vol. 19, no. 4, pp. 2776–2787, 2022.

[12] T. Elmokadem, M. Zribi, and K. Youcef-Toumi, "Trajectory tracking sliding mode control of underactuated auvs," *Nonlinear Dynamics*, vol. 84, pp. 1079–1091, 2016.

[13] A. Wadi, S. Mukhopadhyay, and J.-H. Lee, "A novel disturbance-robust adaptive trajectory tracking controller for a class of underactuated autonomous underwater vehicles," *Ocean Engineering*, vol. 189, p. 106377, 2019.

[14] T. Elmokadem, M. Zribi, and K. Youcef-Toumi, "Terminal sliding mode control for the trajectory tracking of underactuated autonomous underwater vehicles," *Ocean Engineering*, vol. 129, pp. 613–625, 2017.

[15] A. Hackbarth, E. Kreuzer, and E. Solowjow, "Hippocampus: A micro underwater vehicle for swarm applications," in *2015 IEEE/RSJ International Conference on Intelligent Robots and Systems (IROS)*, 2015, pp. 2258–2263.

[16] D. A. Duecker, A. Hackbarth, T. Johannink, E. Kreuzer, and E. Solowjow, "Micro underwater vehicle hydrobatics: A submerged furuta pendulum," in *2018 IEEE International Conference on Robotics and Automation (ICRA)*, 2018, pp. 7498–7503.

[17] K. Yao, N. Bauschmann, T. L. Alff, W. Cheah, D. A. Duecker, K. Groves, O. Marjanovic, and S. Watson, "Image-based visual servoing switchable leader-follower control of heterogeneous multi-agent underwater robot system," in *2023 IEEE International Conference on Robotics and Automation (ICRA)*. IEEE, 2023, pp. 5200–5206.

[18] D. A. Duecker, C. Horst, and E. Kreuzer, "From aerobatics to hydrobatics: Agile trajectory planning and tracking for micro underwater robots," in *2021 IEEE/RSJ International Conference on Intelligent Robots and Systems (IROS)*. IEEE, 2021, pp. 8617–8624.

[19] J. C. Willems, "Dissipative dynamical systems part i: General theory," *Archive for rational mechanics and analysis*, vol. 45, no. 5, pp. 321–351, 1972.

[20] R. Sepulchre, M. Jankovic, and P. V. Kokotovic, *Constructive nonlinear control*. Springer Science & Business Media, 2012.

[21] B. Brogliato, R. Lozano, B. Maschke, O. Egeland, *et al.*, "Dissipative systems analysis and control," *Theory and Applications*, vol. 2, pp. 2–5, 2007.

[22] A. Van der Schaft, *L2-gain and passivity techniques in nonlinear control, 3rd ed.* Springer, 2016.

[23] J. W. Simpson-Porco, "Equilibrium-independent dissipativity with quadratic supply rates," *IEEE Transactions on Automatic Control*, vol. 64, no. 4, pp. 1440–1455, 2019.

[24] D. A. Duecker, E. Kreuzer, G. Maerker, and E. Solowjow, "Parameter identification for micro underwater vehicles," *PAMM*, vol. 18, no. 1, p. e201800350, 2018.

[25] A. Hackbarth, E. Kreuzer, and E. Solowjow, "Hippocampus: A micro underwater vehicle for swarm applications," in *2015 IEEE/RSJ International Conference on Intelligent Robots and Systems (IROS)*, 2015, pp. 2258–2263.